



가 MDCT 가
 : 43
 MDCT , 3 mm
 가 가 가 ,
 가 가 가
 : 214 , 33 (15.4%) 가
 가
 (51.5% 33.3%), (65.7% 87.8% 63.6%)
 79.4%). 가 가
 : , 가 가

가 , 5 (4). , 가 가
 10 - 15% ,
 10,00 0.46 , 21.1% Multidetector computed tomography(MDCT)
 가 (1).
 80% (non - small cell lung cancer: mutliplanar reformation(MPR)
 NSCLC) , (coronal reformatted image)
 , MDCT 가
 (2).
 (computed tomo - graphy: (5 - 7),
 CT) (axial image) 가 MDCT MPR 가
 46 - 87% 69 - 89%, 65 -
 84% (3). , (8, 9).
 가 / MDCT 가
 (PET/CT) 가 가
 가 (10 -
 가
 12). 가

¹가
²가

MDCT 가

MDCT 가

가 , 4 가

가

AJCC(American Joint Committee on Cancer) 1996 (13).

10 mm

2005 4 2007 6 (26) MDCT

43 43

32 (74.4%), 11 (25.6%) , 38

78 , 60.3 (61.84 , 55.82)

3 57 , 18.58 (15.74 , 26.82)

43 42 , 1 (pared T - test) 가 , p - value가 0.05

42 8 가

(pneumonectomy) , 34 (lobectomy) SPSS(ver. 12.0, SPSS, Chicago, U.S.A.)

24 ,

17 , 1

(synchronous primary lung cancer) 20

2

가

43 MDCT(Somatom sensation 64, Siemens Medical Solution, Erlangen, Germany)

120 kVp, 140 mAs, 0.5 sec, 43 (squamous cell carcinoma) 21 (48.83%) 가 (adeno-carcinoma) 12 (27.90%) , (bronchioloalveolar carcinoma), (large cell endocrine carcinoma), (carcinoid tumor)

(slice width) 1 mm, (table feed) 14 43 214

mm/sec, (pitch factor) 1.4 , 90 mL 가 33 ,

3 ml/sec 181 가 43

가 1 21 가 22 ,

1 mm raw data 3 21 가

Rapida 3D(version 2.8, Infinitt, Seoul, Korea) 3 mm , 3 가 33 ,

mm 11 가 ,

(window level) 6 17 가

30 HU, (window width) 400 HU PACS 가

181 159 가

Table 1. Comparison of LN Analysis between Axial Images Alone and Axial and Coronal Reformatted Images per Nodal Groups

	Axial image alone		Axial & Coronal reformatted images		p-value
	10 mm	< 10 mm	10 mm	< 10 mm	
+	11	22	17	16	
-	22	159	62	119	
Total	33	181	79	135	
Sensitivity	11/33 (33.3%)		17/33 (51.5%)		0.135
Specificity	159/181 (87.8%)		119/181 (65.7%)		<0.05
Accuracy	170/214 (79.4%)		136/214 (63.6%)		<0.05

가 , 40
 119 가 (Table 2).
 가 79.41%
 가 33.3% 51.5% 26.47%, 74.36% 33.33% ,
 가 87.8% 65.7% , 79.4% 63.6% 48.00% 93.33% 40.00%, 76.00%
 (Table 1) (Fig. 1, 2).
 가 7 가 25 가 , 2

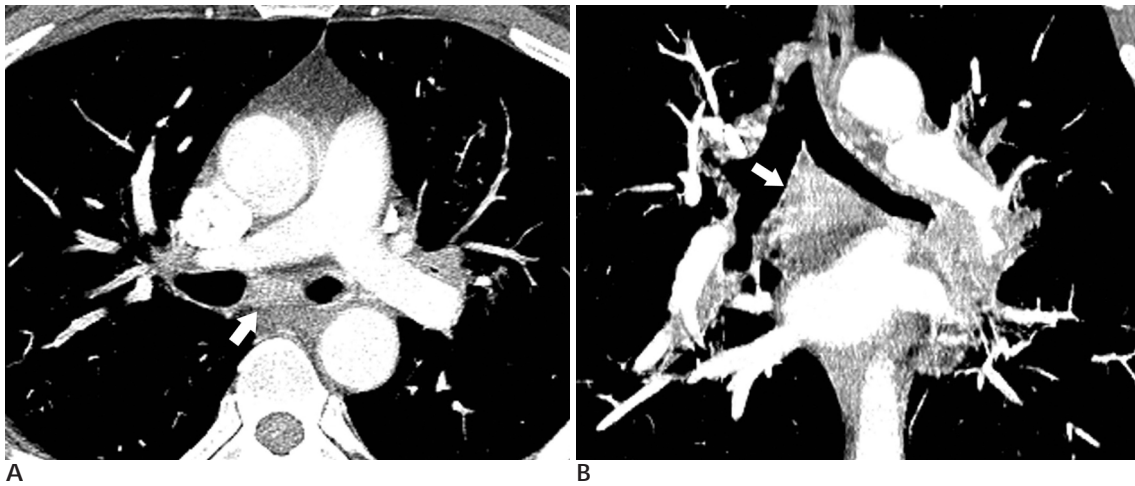


Fig. 1. Squamous cell carcinoma in a 54-year-old man.
A. Axial CT image shows equivocal sized subcarinal LN (arrow), measured 9 mm short-axis diameter.
B. Coronal reformatted CT image demonstrates that it is large enough to be suggested as metastatic LN. (21 mm short-axis diameter) The LN was proven metastasis pathologically.

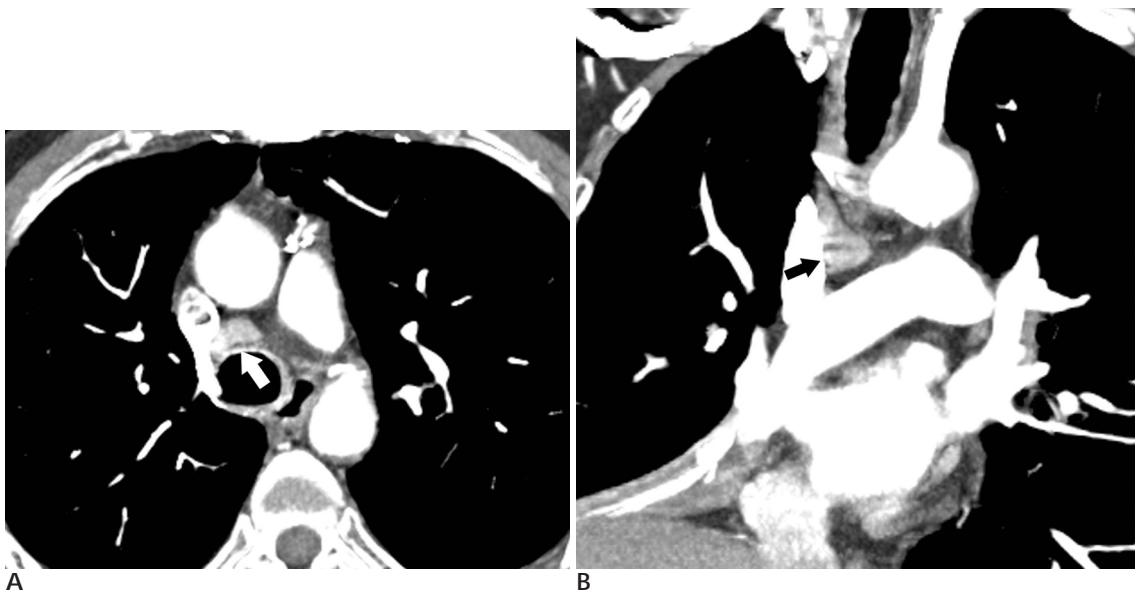


Fig. 2. Squamous cell carcinoma in a 53-year-old man.
A. Axial CT image shows small to equivocal sized LN (arrow) in right lower paratracheal area, measured 8 mm short-axis diameter.
B. Coronal reformatted CT image shows that it is large enough to be suggested as metastatic LN. (16 mm short-axis diameter) But, it was proven reactive node pathologically.

MDCT
 , MPR confidence 1.36 ± 1.14,
 1.56 ± 1.25 ,
 N 1 N 2
 N2
 , N1 , 4 - point scale 가
 가 (10).
 10 Nishino (11) 10 mm 가
 , (upper & lower paratracheal area) 가
 0.71
 (pericardial recess) 0.57
 (Fig. 3). , 7 , Kwan (12) 가
 82% 59%
 가 (11, 12).
 가 가
 MDCT가 MPR 가 가
 MPR 가 가
 . Chooi (10) TNM 가 가
 MPR 가 , 10 mm (14),

Table 2. Comparison of Diagnostic Accuracy to LN Metastasis per Nodal Station between Axial Images Alone and Axial & Coronal Reformatted Images

Nodal station	2R	3	4R	4L	5	6	7	8R	9R	9L	10R	10L	11R	11L
Axial alone	15 /16	6 /6	16 /21	2 /3	12 /14	2 /3	29 /39	2 /2	19 /19	13 /13	8 /16	15 /18	19 /25	12 /19
Axial & coronal	15 /16	6 /6	12 /21	1 /3	12 /14	2 /3	13 /29	0 /2	19 /19	12 /13	5 /16	15 /18	12 /25	12 /19

2 : upper paratracheal LN, 3 : prevascular or retrotracheal LN, 4 : lower paratracheal LN, 5 : subaortic LN, 6 : para-aortic LN, 7 : subcarinal LN, 8 : paraesophageal LN, 9 : pulmonary ligament LN, 10 : hilar LN, 11 : interlobar LN, R : right side, L : left side.

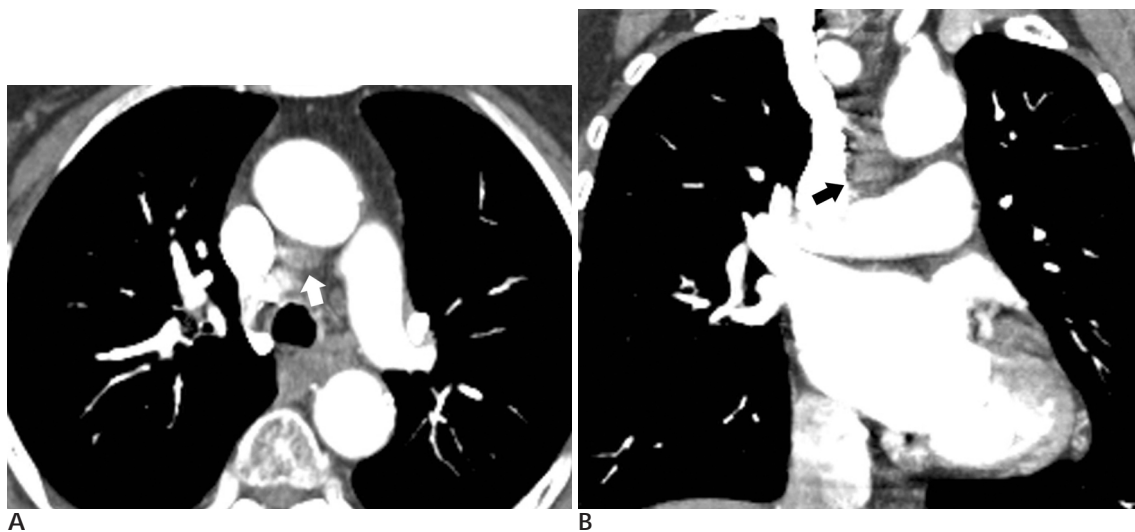


Fig. 3. Adenocarcinoma in a 78-year-old woman.
 A. Axial CT image shows a nodular lesion, suggesting LN (arrow) in lower paratracheal area.
 B. Coronal reformatted CT image shows that it seems to be a superior pericardial recess rather than true LN.

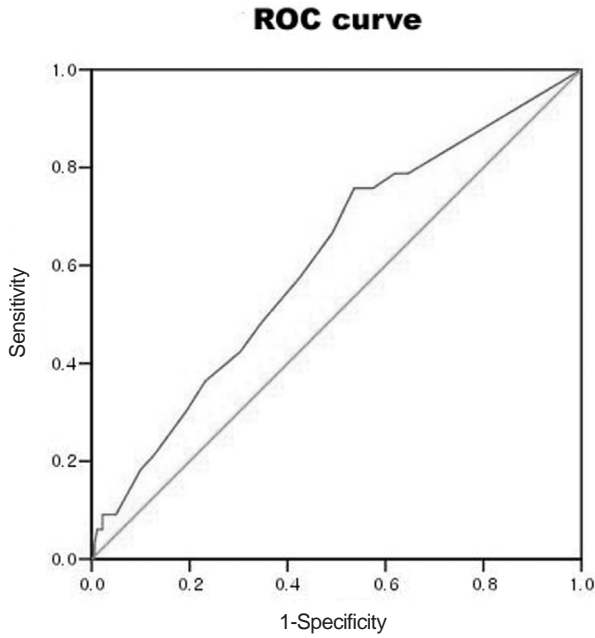
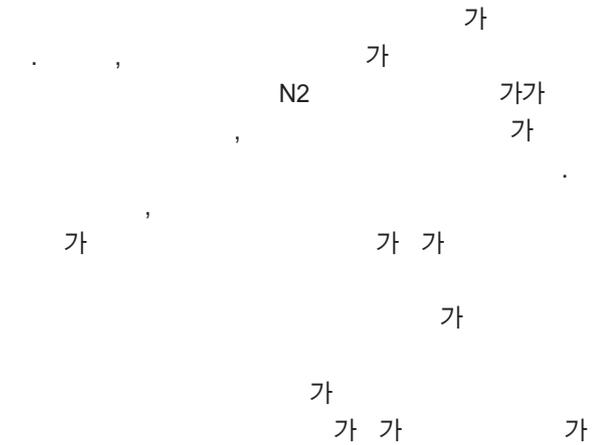
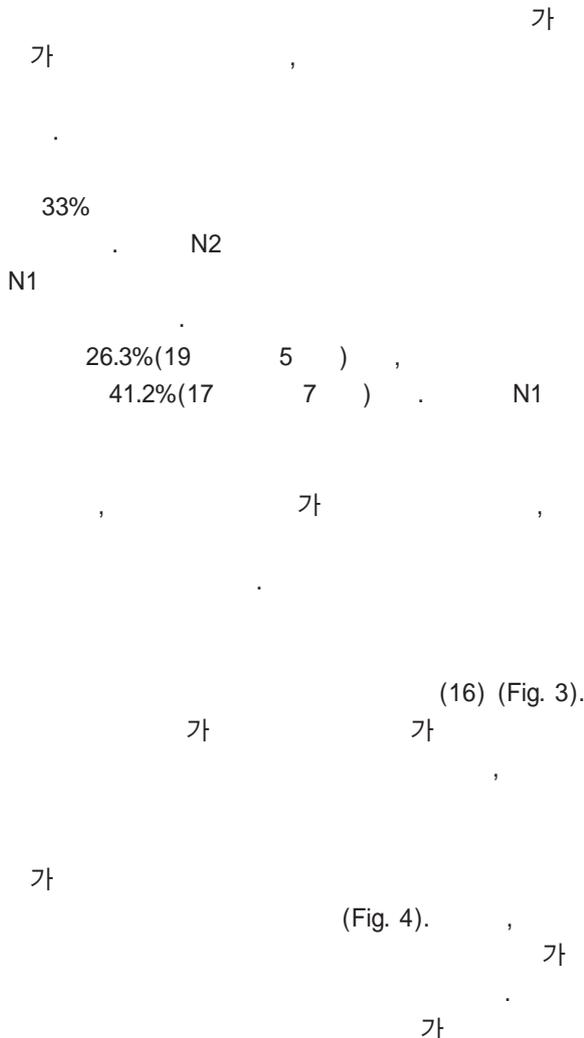


Fig. 5. ROC Curve of LN on Coronal Reformatted Image.

(mediastinoscopic biopsy)



1. Korea National Statistical Office, Annual Report on the Cause of Death Statistics. Taejon: Korea National Statistical Office, Each year
2. Kim ES, Bosquee L. The importance of accurate lymph node staging in early and locally advanced Non-small cell lung cancer: an update on available techniques. *J Thorac Oncol* 2007;2 Suppl 2: S59-S67
3. Chern MS, Wu MH, Chang CY. CT and MRI for staging of locally advanced non-small cell lung cancer. *Lung Cancer* 2003; 42 Suppl 2:S5-S8
4. Yi CA, Lee KS, Kim BT, Shim SS, Chung MJ, Sung YM, et al. Efficacy of helical dynamic CT versus integrated PET/CT for detection of mediastinal nodal metastasis in non-small cell lung cancer. *AJR Am J Roentgenol* 2007;188:318-325
5. Nishino M, Kubo T, Kataoka ML, Gautam S, Raptopoulos V, Hatabu H. Evaluation of pulmonary embolisms using coronal reformations on 64-row multidetector-row computed tomography: comparison with axial images. *J Comput Assist Tomogr* 2006;30: 233-237
6. Remv-Jardin M, Campistrion P, Amara A, Mastora I, Tillie-Leblond I, Delannoy V, et al. Usefulness of coronal reformations in the diagnostic evaluation of infiltrative lung disease. *J Comput Assist Tomogr* 2003;27:266-273
7. Sung YM, Lee KS, Yi CA, Yoon YC, Kim TS, Kim S. Additional coronal reformatted images using low-milliamperage multidetector-row computed tomography: effectiveness in the diagnosis of bronchiectasis. *J Comput Assist Tomogr* 2003;27:490-495
8. Chen CY, Hsu JS, Wu DC, Kang WY, Hsieh JS, Jaw TS, et al. Gastric cancer: preoperative local staging with 3D multi-detector row CT--correlation with surgical and histopathologic results. *Radiology* 2007;242:472-482
9. Filippone A, Ambrosini R, Fuschi M, Marinelli T, Genovesi D, Bonomo L. Preoperative T and N staging of colorectal cancer: accuracy of contrast-enhanced multi-detector row CT colonography--initial experience. *Radiology* 2004;231:83-90
10. Chooi WK, Matthews S, Bull MJ, Morcos SK. Multislice computed tomography in staging lung cancer: the role of multiplanar image reconstruction. *J Comput Assist Tomogr* 2005;29:357-360
11. Nishino M, Kubo T, Kataoka ML, Gautam S, Raptopoulos V,

- Hatabu H. Evaluation of thoracic abnormalities on 64-row multi-detector row CT: comparison between axial images versus coronal reformations. *Eur J Radiol* 2006;59:33-41
12. Kwan SW, Partik BL, Zinck SE, Chan FP, Kee ST, Leung AN, et al. Primary interpretation of thoracic MDCT images using coronal reformations. *AJR Am J Roentgenol* 2005;185:1500-1508
13. Ko JP, Drucker EA, Shepard JA, Mountain CF, Dresler C, Sabloff B, et al. CT depiction of regional nodal stations for lung cancer staging. *AJR Am J Roentgenol* 2000;174:775-782
14. Kiyono K, Sone S, Sakai F, Imai Y, Watanabe T, Izuno I, et al. The number and size of normal mediastinal lymph nodes: a post-mortem study. *AJR Am J Roentgenol* 1988;150:771-776
15. Lee JH, Lee KS, Kim TS, Yi CA, Cho JM, Lee MH. Mediastinal and hilar lymphadenopathy : cross-referenced anatomy on axial and coronal reformatted images displayed by using multi-detector row CT. *J Korean Radiol Soc* 2003;49:285-293
16. Truong MT, Erasmus JJ, Gladish GW, Sabloff BS, Marom EM, Madewell JE, et al. Anatomy of pericardial recesses on multidetector CT: implications for oncologic imaging. *AJR Am J Roentgenol* 2003;181:1109-1113

Value of Coronal Reformatted Images Using Multi-detector Computed Tomography for Nodal Staging in Non Small Cell Lung Cancer Cases¹

Young Sup Shim, M.D., Soo Jin Choi, M.D., Chul Hi Park, M.D., Jae Ik Lee, M.D.²,
Hyung Sik Kim, M.D., Chul Hyun Park, M.D.²

¹Department of Radiology, Gachon University, Gil Medical Center

²Department of Thoracic & Cardiovascular Surgery, Gachon University, Gil Medical Center

Purpose: The aim of our study was to evaluate the value of coronal reformatted images using multi-detector computed tomography (MDCT) imaging in non small cell lung cancer (NSCLC) for the determination of lymph node (LN) metastasis.

Materials and Methods: Chest CT scans using MDCT were performed in 43 patients with pathologically proven NSCLC. The images were reconstructed with a 3 mm thickness in the axial and coronal planes. The axial images were examined for LN metastasis with and without the coronal reformatted images by the consensus of two radiologists on two separate occasions.

Results: In total, 214 nodal groups were dissected, of which, 33 (15.4%) were pathologically proven as LN metastasis. The sensitivity of diagnosis was higher when assessing both the axial and coronal reformatted images compared to the axial images alone (51.5% vs. 33.3%), whereas the specificity and accuracy was lower when examining both the axial and coronal reformatted images (65.7% vs. 87.8% and 63.6% vs. 79.4%). Despite this, the additional coronal reformatted images provided additional anatomical information which was helpful in the assessment of accurate nodal stations and the decline of the pitfalls.

Conclusion: The value of coronal reformatted images for the diagnosis of nodal metastasis in NSCLC may still be unclear; however, the coronal reformatted images may lend support to the axial images in being able to provide additional anatomical information.

Index words : Carcinoma, non small cell lung
Neoplasm staging, lymph nodes
Tomography scanner, multi-detector CT
Radiographic image interpretation, computer-assisted

Address reprint requests to : Soo Jin Choi, M.D., Department of Radiology, Gachon University, Gil Medical Center,
1198, Guwol-dong, Namdong-gu, Incheon, 405-760, Korea
Tel. 82-32-460-3057 Fax. 82-32-460-3065 E-mail: drchoi126@hanmail.net